



## Discover Generics

Cost-Effective CT & MRI Contrast Agents



WATCH VIDEO

# AJNR

## Does Arterial Flow Rate Affect the Assessment of Flow-Diverter Stent Performance?

H.G. Morales, O. Bonnefous, A.J. Geers, O. Brina, V.M. Pereira, L. Spelle, J. Moret and I. Larrabide

This information is current as of June 17, 2025.

*AJNR Am J Neuroradiol* 2016, 37 (12) 2293-2298

doi: <https://doi.org/10.3174/ajnr.A4933>

<http://www.ajnr.org/content/37/12/2293>

# Does Arterial Flow Rate Affect the Assessment of Flow-Diverter Stent Performance?

 H.G. Morales,  O. Bonnefous,  A.J. Geers,  O. Brina,  V.M. Pereira,  L. Spelle,  J. Moret, and  I. Larrabide

## ABSTRACT

**BACKGROUND AND PURPOSE:** Our aim was to assess the performance of flow-diverter stents. The pre- and end-of-treatment angiographies are commonly compared. However, the arterial flow rate may change between acquisitions; therefore, a better understanding of its influence on the local intra-aneurysmal hemodynamics before and after flow-diverter stent use is required.

**MATERIALS AND METHODS:** Twenty-five image-based aneurysm models extracted from 3D rotational angiograms were conditioned for computational fluid dynamics simulations. Pulsatile simulations were performed at different arterial flow rates, covering a wide possible range of physiologic flows among 1–5 mL/s. The effect of flow-diverter stents on intra-aneurysmal hemodynamics was numerically simulated with a porous medium model. Spatiotemporal-averaged intra-aneurysmal flow velocity and flow rate were calculated for each case to quantify the hemodynamics after treatment. The short-term flow-diverter stent performance was characterized by the relative velocity reduction inside the aneurysm.

**RESULTS:** Spatiotemporal-averaged intra-aneurysmal flow velocity before and after flow-diverter stent use is linearly proportional to the mean arterial flow rate (minimum  $R^2 > 0.983$  of the linear regression models for untreated and stented models). Relative velocity reduction asymptotically decreases with increasing mean arterial flow rate. When the most probable range of arterial flow rate was considered (3–5 mL/s), instead of the wide possible flow range, the mean SD of relative velocity reduction was reduced from 3.6% to 0.48%.

**CONCLUSIONS:** Both intra-aneurysmal aneurysm velocity and flow-diverter stent performance depend on the arterial flow rate. The performance could be considered independent of the arterial flow rates within the most probable range of physiologic flows.

**ABBREVIATIONS:** CFD = computational fluid dynamics;  $m$  = ratio between the aneurysm velocity and the arterial flow;  $\bar{Q}$  = mean arterial flow rate;  $Q_{\min}$  = minimum arterial flow rate required to have a distinguishable velocity inside the aneurysm;  $s$  = stented;  $u$  = untreated;  $vel_{\text{red}}$  = relative velocity reduction;  $vel_{\text{sa}}$  = spatiotemporal-averaged flow velocity

Flow diverters are low-porosity stents designed to reduce the blood flow inside the aneurysm cavity. They also serve as a scaffold for neointima formation at the aneurysm ostium.<sup>1,2</sup> To evaluate the potential occlusion performance by intrasaccular

thrombus formation, one must conduct middle- and long-term observations. However, to foresee these future conditions and to assess potential short-term complications, one must evaluate immediate posttreatment hemodynamic features using the end-of-treatment angiography.<sup>3–5</sup>

Qualitative, angiography-based metrics of short-term hemodynamics have been proposed, such as the SMART (simple measurement of aneurysm residual after treatment) scale or grading of the intrasaccular contrast flow speed.<sup>6,7</sup> Additionally, more complex quantitative techniques have been introduced by processing the pre- and posttreatment angiograms.<sup>8</sup> In most of these techniques, information about the contrast propagation is directly compared between pre- and posttreatment angiograms without paying attention to the potential arterial flow rate changes between image acquisitions and its impact on aneurysmal hemodynamics. It has been reported that change in 30%–50% of

Received November 19, 2015; accepted after revision July 20, 2016.

From Medisys-Philips Research (H.G.M., O.Bonnefous), Paris, France; Centre for Cardiovascular Science (A.J.G.), University of Edinburgh, Edinburgh, Scotland; Department of Information and Communication Technologies (A.J.G.), Universitat Pompeu Fabra, Barcelona, Spain; Department of Information Neuroradiology (O.Brina), University Hospital of Geneva, Geneva, Switzerland; Department of Medical Imaging and Department of Surgery (V.M.P.), University Health Network, Toronto, Ontario, Canada; Interventional Neuroradiology (L.S., J.M.), Beaujon University Hospital, Clichy, France; Paris Diderot University (L.S.), Paris, France; and PLADEMA-CONICET (I.L.), Universidad Nacional del Centro de la Provincia de Buenos Aires, Tandil, Argentina.

Please address correspondence to Hernán G. Morales, PhD, 33 Rue de Verdun, 92156 Suresnes, France; e-mail: hernan.morales@philips.com

<http://dx.doi.org/10.3174/ajnr.A4933>

the mean arterial flow rate could lead to a 30%–80% variation of hemodynamic quantities, such as mean flow velocity, aneurysm inflow, or wall shear stress.<sup>9</sup>

The purpose of this study was to evaluate the role of the arterial flow rate on flow-diverter stent performance. Because patient-specific flow measurements are not unique and depend on the instance at which a medical examination is performed, a wide range of flow rates was considered.

## MATERIALS AND METHODS

Twenty-five aneurysms from different patients were investigated. 3D rotational angiography images of the aneurysms and their surrounding vasculature were acquired with an x-ray system (Al-lura Xper FD20; Philips Healthcare, Best, the Netherlands). All aneurysms were located between the siphon of the internal carotid artery and its downstream bifurcation. Medical data were collected by 2 departments of interventional neuroradiology: University Hospitals of Geneva, Geneva, Switzerland, and Beaujon University Hospital, France.

From these images, a surface mesh was extracted by image segmentation. The surface meshes were cleaned and smoothed. Hexahedral meshes inside each vascular model were generated with a cell size of 0.2 mm at the wall, 0.1 mm in the porous medium, and 0.2 mm elsewhere, with 4 cells between sizes. The total number of elements ranged between  $2.08 \times 10^5$  and  $6.44 \times 10^5$ . For a given case, the same mesh was used for both untreated and stented models. More details about the mesh strategies can be found elsewhere.<sup>10–12</sup>

In these volumetric meshes, governing equations of flow motion were solved by using the open-source computational fluid dynamics (CFD) package OpenFOAM 2.2.1 (www.openfoam.org). Arterial walls were considered rigid and nonslippery (flow velocity = 0). Blood was modeled as a Newtonian and incompressible fluid, with the knowledge that changes in blood viscosity due to increments in shear strain rates can be neglected.<sup>13</sup> A parabolic profile was set at the inlet of each vascular model as a spatial condition, which changes in time according to the pulsatile waveform (temporal variation). Zero-pressure conditions were imposed at all outlets. Details of this methodology can be found elsewhere.<sup>10</sup>

### Arterial Flow Rates

To single out the effect of the mean arterial flow rate,  $\bar{Q}$ , the same shape of the flow waveform was used for all simulations, which was scaled to achieve the desired  $\bar{Q}$  (Fig 1). The waveform was originally extracted from a DSA sequence of a patient by using valid optical flow techniques.<sup>14–16</sup> Per case, 9 pulsatile flow simulations were created. Five of those flows were set within the most probable range (3 mL/s to 5 mL/s),<sup>17,18</sup> every 0.5 mL/s. To cover lower flows, which occurs according to a possible range among 1 mL/s to 5 mL/s, we used both the inlet-area flow condition<sup>19</sup> and the 1.5-Pa wall shear stress condition at the inlet. In case those strategies provided a value within 3 mL/s to 5 mL/s, flow rate values were imposed at 1.0, 1.5, 2.0, and 2.5 mL/s.<sup>10</sup> With this configuration, the highest simulated flow rate has a systolic value of 7.56 mL/s, which is below the highest values measured in patients (>11 mL/s).<sup>17</sup>

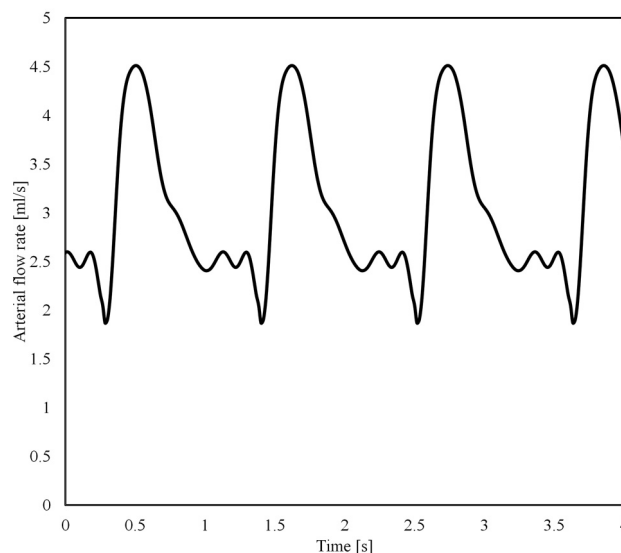


FIG 1. Waveform ( $\bar{Q} = 3$  mL/s).

### Virtual Stent Placement

To model the influence of a flow-diverter stent on the intra-aneurysmal hemodynamics, we placed a porous medium at the aneurysm ostium. This medium locally imposes an additional hydraulic resistance to flow and has been previously used.<sup>11,20–23</sup> The Darcy-Forchheimer law was used in the porous medium, which includes both viscous- and inertia-related pressure losses. The parameters of this medium used were  $k = 8.7 \times 10^{-7}$  (viscosity term) and  $F = 8.1 \times 10^4$  (inertia term), and an equivalent porosity of around 70% was imposed. Details of the volumetric porous medium approach can be found elsewhere.<sup>11</sup>

### Data Analysis

The following analysis was conducted to characterize the flow-diverter stent performance at different arterial flow rates.

Inside the aneurysm, the spatiotemporal-averaged flow velocity,  $\overline{vel}_{sa}$ , was calculated, which has been shown to be independent of the waveform shape.<sup>12,24</sup> Per case, linear regression models were applied to the untreated and stented datasets. The goal was to confirm that  $\overline{vel}_{sa}$  can be characterized as a linear function of  $\bar{Q}$  (see Equation 1) for untreated aneurysms<sup>12</sup> and to extend this characterization of the  $\overline{vel}_{sa}$  after treatment under the hypothesis that this relationship should be preserved.

$$1) \quad \overline{vel}_{sa}(\bar{Q}) = m \cdot (\bar{Q} - Q_{min})$$

In Equation 1, the parameters  $m$  and  $Q_{min}$  are given by the linear regression models applied on the results of the CFD simulations, but they can also be derived from measurements by using functional image analysis.<sup>14,15</sup>  $Q_{min}$  can be interpreted as the minimum arterial flow rate required to have a distinguishable velocity inside the aneurysm. The parameter  $m$  represents the ratio between the aneurysm velocity and the arterial flow.

Afterward, the flow-diverter stent performance was characterized by the relative velocity reduction,  $vel_{red}$ :

$$2) \quad vel_{red} = 1 - \frac{\overline{vel}_{sa,s}}{\overline{vel}_{sa,u}}$$

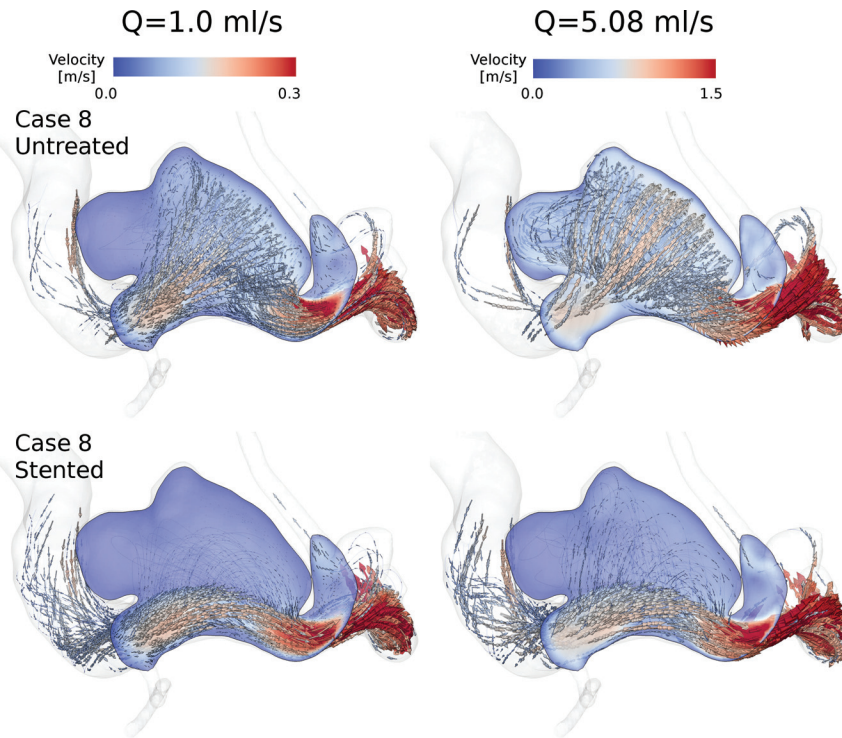


**FIG 2.** Peak systolic instantaneous streamlines of velocity and an aneurysmal cut plane for case 8 at 2 arterial flow rates. Untreated and stented models are in the upper and lower rows, respectively.

#### Linear regressions for untreated and stented conditions for all aneurysm models

Case	Untreated			Stented		
	$m$	$Q_{\min}$	$R^2$	$m$	$Q_{\min}$	$R^2$
1	0.025	0.484	1.000	0.006	0.929	0.997
2	0.037	0.395	1.000	0.010	0.816	0.994
3	0.053	0.588	0.999	0.012	0.770	0.996
4	0.047	0.330	1.000	0.018	0.605	0.997
5	0.070	0.508	0.999	0.015	0.762	0.994
6	0.043	0.325	1.000	0.011	0.895	0.992
7	0.075	0.477	0.995	0.024	0.891	0.983
8 <sup>a</sup>	0.069	0.451	1.000	0.019	0.461	0.999
9	0.067	0.664	0.997	0.015	1.062	0.990
10	0.026	0.255	0.998	0.008	0.744	0.993
11 <sup>a</sup>	0.091	0.356	1.000	0.022	0.368	0.999
12	0.047	0.484	1.000	0.016	1.075	0.983
13	0.030	0.591	0.998	0.011	1.053	0.991
14	0.048	0.394	1.000	0.022	0.588	0.997
15	0.104	0.364	1.000	0.030	0.677	0.992
16	0.041	0.580	0.999	0.014	0.764	0.996
17	0.051	0.676	0.999	0.013	1.038	0.983
18	0.060	0.353	1.000	0.017	0.672	0.998
19	0.047	0.365	1.000	0.007	0.946	0.990
20	0.078	0.540	0.999	0.015	0.974	0.990
21	0.038	0.231	1.000	0.009	0.473	1.000
22 <sup>a</sup>	0.112	0.282	1.000	0.058	0.333	1.000
23	0.040	0.454	1.000	0.025	0.706	0.996
24	0.067	0.439	0.999	0.027	0.745	0.994
25	0.025	0.201	1.000	0.011	0.679	0.999

<sup>a</sup> Cases in the row have  $\Delta Q_{\min} \leq 0.05$  mL/s.

where the indexes  $u$  and  $s$  stand for untreated and stented, respectively. By placing Equation 1 inside Equation 2 for both untreated and stented conditions, defining the slope ratio  $r_m = m_s / m_u$ , and making  $\bar{Q}_s = \bar{Q}_u = \bar{Q}$ , Equation 2 becomes:

$$3) \quad vel_{red} = 1 - r_m \cdot \frac{(\bar{Q} - Q_{\min,s})}{(\bar{Q} - Q_{\min,u})}.$$

To evaluate when  $vel_{red}$  becomes independent of the flow rate, Equation 3 was derived with respect to  $\bar{Q}$  and set to zero:

$$4) \quad \frac{\partial(vel_{red})}{\partial \bar{Q}} = \frac{-r_m \cdot \Delta Q_{\min}}{(\bar{Q} - Q_{\min,u})^2} = 0,$$

where  $\Delta Q_{\min} = Q_{\min,s} - Q_{\min,u}$ . Equation 4 is satisfied under 2 conditions:

- The ratio  $r_m$  is zero, meaning that the slope after stent placement ( $m_s$ ) is zero or “tiny” with respect to the slope before treatment ( $m_u$ ), ie,  $m_u \gg m_s$ .
- $\Delta Q_{\min} = 0$ , meaning that the  $Q_{\min}$  before and after stent placement are the same ( $Q_{\min,s} \approx Q_{\min,u}$ ).

A less-evident third condition may occur in the case that both,  $Q_{\min,s}$  and  $Q_{\min,u}$  (in Equation 3), are small compared with  $\bar{Q}$ . In this situation, equation 3 becomes

$$5) \quad vel_{red} = 1 - r_m.$$

## RESULTS

In all cases, flow direction was changed after treatment. The porous medium produced an additional hydraulic resistance to flow near the aneurysm ostium, thus reducing the amount of flow that penetrates the aneurysm. Figure 2 shows examples of the flow patterns that can be obtained after flow diversion by using a porous medium. These results are similar to those using explicit stent models.<sup>25–27</sup> In general, it seems that the flow patterns were unaltered when  $\bar{Q}$  was changed.

$\bar{vel}_{sa}$  linearly increased when  $\bar{Q}$  goes up before and after treatment for all cases (minimum  $R^2 > 0.995$  for untreated and  $R^2 > 0.983$  for stented cases). The Table presents the results of the linear regressions that were applied for each case before and after treatment. Moreover for all cases, the slope  $m$  was reduced ( $r_m < 1$ ) and  $Q_{\min,s} > Q_{\min,u}$  ( $\Delta Q > 0$ ) after flow-diverter stent placement. Figure 3 depicts the  $\bar{vel}_{sa}$  as a function of  $\bar{Q}$  for cases 1 and 8 as a visual example of these results. Using these linear regressions, we calculated  $vel_{red}$  (Equation 3) and plotted it in Fig 4 by using the range (1–6 mL/s).

In general,  $vel_{red}$  decreased with an increasing arterial flow rate (Fig 4A). However in cases 8, 11, and 22 (footnoted in the Table), almost a constant reduction was observed. In those cases,  $\Delta Q_{\min}$  was relatively small (mean = 0.024 mL/s, maximum  $\leq 0.05$  mL/s) compared with the rest of the cases (mean = 0.37 mL/s, minimum  $\geq 0.18$  mL/s). These results can also be visualized in Fig 4B, where the standard deviation of  $vel_{red}$  is presented for each case. When the most probable flow range is taken into account at 3–5 mL/s,<sup>17,18</sup> the mean SD of  $vel_{red}$  was reduced from 3.6% (Fig 4B) to 0.48% (Fig 4C).

## DISCUSSION

In this study, the intra-aneurysmal hemodynamics were investigated before and after flow-diverter stent placement for different arterial flow rates in 25 aneurysm models. As was expected,  $\overline{vel}_{sa}$  increases when the arterial flow rate goes up (Fig 3). However, the increment is linear and can be simply represented by 2 coefficients:  $m$  and  $Q_{min}$ . When the short-term flow-diverter stent performance is characterized by the relative reduction of the aneurysm flow velocity,  $vel_{red}$  (Equation 3), the flow-diverter stent was relatively “more effective” at lower flow rates than at higher ones (Fig 4). To better understand these findings, we performed the following analyses.

### Linear Law

It was confirmed in untreated aneurysm models that the  $\overline{vel}_{sa}$  linearly depends on  $\overline{Q}$  ( $R^2 > 0.995$ ),<sup>12</sup> and this linear relationship was extended for stented aneurysms ( $R^2 > 0.983$ ). Indeed, from a hemodynamic point of view, a stented aneurysm is like another aneurysm with a particular resistance near the ostium (obtained by the stent), and this law is preserved. This relationship is very useful for characterizing aneurysm flow velocities because the influence of the arterial flow rate is included. Other variables such as wall shear stress or pressure can be also represented as functions of  $\overline{Q}$ , but a quadratic relation seems to be more appropriate according to previous studies.<sup>12,24</sup> These characterizations go beyond any hemodynamic assessment by using patient-specific measure-

ments (either from CFD simulations or from image processing), because those evaluations are limited to flow conditions during recording, which change with time.

This linear law describes the intra-aneurysmal velocity at any flow rate in terms of the slope  $m$  and  $Q_{min}$  (both positive). If the endovascular device reduced the aneurysmal velocity, 2 changes were observed in these curves. First, the slope after treatment must be smaller than before (yet still positive), making  $r_m < 1$ . This ratio is a direct indication that the blood flow speed is decreased after treatment, with the benefit of being independent of the arterial flow rate. For example,  $r_m$  can be used to compare devices for a given aneurysm because it is related to the untreated condition, and a lower  $r_m$  means that the implanted device will produce a higher velocity reduction inside the aneurysm. On the contrary,  $r_m > 1$  means that the treatment is actually increasing the velocity inside the aneurysm, which could be harmful and may increase the risk of rupture.

The slopes can also be used to compare cases because they quantify the hemodynamics of each aneurysm, independent of the arterial flow rate. For example, a standardized “critical slope” after flow diversion can be identified, in which aneurysm thrombosis would be expected. Nevertheless, further investigation is required to find this critical slope in a larger dataset with clinical follow-up information. Still, if these curves are used for this purpose or another one such as aneurysm rupture, then the specific arterial flow rate at which those aneurysms were evaluated becomes irrelevant because the flow rate is implicitly considered when using this approach.

The second change in the curves is that  $Q_{min}$  increases after stent placement; this change makes a positive  $\Delta Q_{min}$  ( $Q_{min,s} - Q_{min,u}$ ). As discussed by Morales and Bonnefous,<sup>12</sup>  $Q_{min}$  is given by the regressions and does not necessarily represent a physical phenomenon (zero velocity for a given nonzero flow rate), though it can be seen as the minimum arterial flow rate required to have a distinguishable flow motion inside the aneurysm cavity.  $Q_{min}$  increases after stent placement because the blood flow needs more energy (a higher  $Q_{min}$ ) to overcome the additional hydraulic

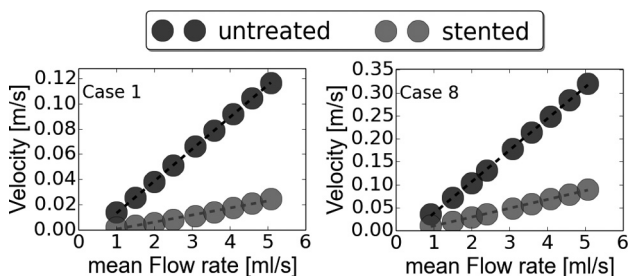


**FIG 3.**  $\overline{vel}_{sa}$  for cases 1 and 8 before and after flow-diverter stent placement. Points were derived from CFD simulations, and the curves represent the linear regressions that were applied on each point set.

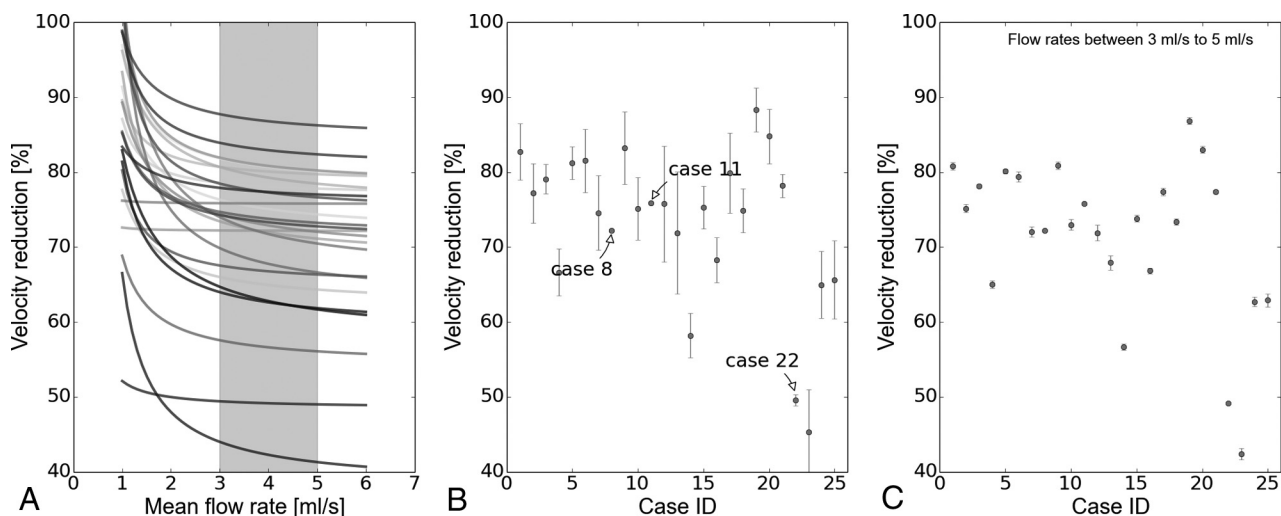


**FIG 4.** A,  $vel_{red}$  as function of  $\overline{Q}$ , where the gray region represents the most probable arterial flow range (3–5 mL/s). B, Mean and SD of  $vel_{red}$  per case. C, Mean and SD of  $vel_{red}$  per case but only considering the most probable arterial flow range.  $vel_{red}$  is presented as a percentage.



resistance produced by the flow-diverter stent and then to generate this distinguishable flow motion.

The validity of the linear model is only within the possible flow rate range studied here, which includes the most probable physiologic range. For flow rates between 0 and 1.0 mL/s, a quadratic model crossing the origin would be more appropriate. Nevertheless, the interest in such a low range is arguable because it will not be a physiologic condition and other phenomena, such as blood coagulation, may arise. Moreover, because the flow rate range covered here is based on the variability among patients,<sup>19</sup> a shorter patient-specific flow range should be within this wide range without affecting the presented relationships for that patient.

### Flow-Diverter Stent Performance and Arterial Flow Rate

In this study, the short-term flow-diverter stent performance was characterized by  $vel_{red}$ .

As presented in Equation 3 and confirmed in Fig 4,  $vel_{red}$  is higher when the arterial flow rate is low. This finding indicates that the arterial flow rate should be taken into account to fairly compare the performance of endovascular devices by any approach (in vivo, in vitro, or in silico). Using the same Reynolds number would not be fair for comparing the hemodynamics of 2 (or more) aneurysms because this number depends on the local arterial caliber; therefore, if 2 cases have the same number, the one with the higher arterial caliber will have a lower flow rate. This lower arterial flow rate benefits the device performance as shown in Fig 4A.

The weakening of the stent performance when increasing the arterial flow rate (and vice versa) is because the hydraulic resistance of the flow-diverter stent decreases when increasing the Reynolds number (proportional to the flow rate). This phenomenon is well-known in classic fluid mechanics and has been thoroughly studied for high-porosity stent placement in cerebral aneurysms.<sup>25</sup>

Previously, Larrabide et al<sup>26</sup> performed CFD simulations by using an explicit representation of the flow-diverter stents to investigate the velocity variation during the cardiac cycle as a mean to quantify the device performances. They found that the pulsatility of the aneurysmal velocity increases after treatment. Similarly, Peach et al<sup>27</sup> investigated the influence of several flow-diverter stent designs (different porosities and pore sizes) on hemodynamics, and the lowest flow reductions were seen at peak systole, when parent vessel flow is at its highest. These studies show that the stent performance is “weaker” at systole than at diastole (higher-versus-lower arterial flow rates); this finding is congruent with our findings when increasing the arterial flow rates.

Additionally, Mut et al<sup>9</sup> varied the flow rate conditions before and after flow-diverter stent placement. It was found that a change in 30%–50% of the mean arterial flow could lead to a variation between 30% and 80% of some hemodynamic quantities. This is similar to the presentation in Fig 3—that is, variations of  $\bar{Q}$  do change  $\overline{vel}_{sa}$ . Besides, the authors concluded that this variation can lead to misleading interpretations when clinical information is used, in particular, when pre- and posttreatment conditions are compared because flow conditions may vary

among image acquisitions. The results presented here are in accordance with this statement, and the authors stress that caution is needed when comparing the 2 situations (either experimental or clinical) in which the arterial flow rates are known.

### Flow Rate–Free Performance

The first condition that satisfies Equation 4 was not found in our study because it means flow cessation inside the aneurysm after treatment ( $m_s = 0$ ), which can be achieved after several months due to the formation of intrasaccular thrombus. The second condition was observed in 3 cases. There,  $\Delta Q_{min}$  was very small ( $\leq 0.05$  mL/s) compared with the rest of the cases (minimum  $\geq 0.018$  mL/s).

The third condition that makes  $vel_{red}$  independent of  $\bar{Q}$  is the one derived from Equation 5. The largest variations in  $vel_{red}$  were observed at the lower end of the possible flow range, which are outside the most probable range at the ICA (gray region in Fig 4A). Nevertheless, further investigation is required in a larger population to see for which cases this assumption is plausible, by measuring the SD of  $vel_{red}$ , for example. A possible case stratification could be based on morphologic features such as aneurysm size and shape.

### Potential Clinical Translation

Equation 5 is a plausible way to transfer these findings into clinical practice. However, this equation assumes that  $\bar{Q}_s = \bar{Q}_u = \bar{Q}$  and that  $\bar{Q} \gg Q_{min}$  (for untreated and stented conditions).

To overcome the first limitation, (ie,  $\bar{Q}_s \neq \bar{Q}_u$ ), a more general expression should be used:

$$6) \quad vel_{red} = 1 - r_m \cdot \frac{\bar{Q}_s}{\bar{Q}_u}$$

Equation 6 states that  $vel_{red}$  can be obtained by knowing  $r_m$ , the arterial flow rate before ( $\bar{Q}_u$ ) and after treatment ( $\bar{Q}_s$ ) and that those  $\bar{Q}$ 's should be higher to neglect the influence of each  $Q_{min}$ . These quantities can be obtained from either CFD simulations or image analysis. For the latter, medical images can be processed by using optical flow techniques to retrieve both the arterial and aneurysm flows.<sup>14–16</sup>

From a more generic perspective, this study reveals the importance of the arterial flow rate when evaluating aneurysm hemodynamics. As a consequence, qualitative evaluations such as the SMART scale or the grading of contrast flow speed should be avoided because no distinction can be made between variations in contrast due to either the implanted device or a reduction in the arterial flow rate. This advice is very important when comparing pre- and posttreatment angiograms of the same patient, but also when comparing among subjects. Additionally, this study proposes a simple quantification approach in which the arterial flow rate is considered to properly quantify aneurysm hemodynamics.

### Limitations

Arterial walls were considered a rigid wall though it is known that the arteries are flexible structures and radial dilations occur due to pressure changes. Nevertheless, it is expected that main flow structures will be preserved.<sup>28</sup> As in both numeric and experimental studies, the vascular morphology was not altered after flow-

diverter stent placement. Indeed, the placement of a stent could locally change the artery shape. Unfortunately, it is not possible to overcome this limitation due to the lack of information regarding the mechanical properties of the artery and implanted devices, as well as the surrounding tissue and organs that could influence the final morphology after stent placement.

## CONCLUSIONS

Spatiotemporal-averaged intra-aneurysmal velocity can be characterized by a linear function of the arterial flow rate before and after flow-diverter stent placement. This characterization provides a simple way to study intra-aneurysmal hemodynamics that goes beyond any patient-specific flow measurements. By using this linear relationship, it was found that the arterial flow rate affects the short-term flow-diverter stent performance. However, the device performance can be considered independent of the arterial flow rates within (and above) the physiologic flow range.

## ACKNOWLEDGMENTS

We thank the units of interventional neuroradiology of the Department of Medical Imaging and Information Sciences, University Hospitals of Geneva, Switzerland, and of Beaujon University Hospital, Clichy, France, for providing the medical images from which the vascular models were extracted.

Disclosures: Vitor Mendes Pereira—UNRELATED: Grant: Philips Healthcare.\* Comments: grant to pay for a technician for 2 years for a related research project. Laurent Spelle—UNRELATED: Consulting Fee or Honorarium: Medtronic, Stryker, Sequent Medical. Jacques Moret—UNRELATED: Consultancy: Covidien, MicroVention, Stryker. Ignacio Larrabide—UNRELATED: Consultancy: Galgo Medical S.L.; Employment: CONICET and UNICEN; Patents (planned, pending or issued): WO 2015063352 A1. \*Money paid to the institution.

## REFERENCES

1. Durso PI, Lanzino G, Cloft HJ, et al. **Flow diversion for intracranial aneurysms: a review.** *Stroke* 2011;42:2363–68 [CrossRef Medline](#)
2. Pierot L. **flow diverter stents in the treatment of intracranial aneurysms: where are we?** *J Neuroradiol* 2011;38:40–46 [CrossRef Medline](#)
3. Byrne JV, Beltechi R, Yarnold JA, et al. **Early experience in the treatment of intra-cranial aneurysms by endovascular flow diversion: a multicentre prospective study.** *PLoS One* 2010;5:1–8 [CrossRef Medline](#)
4. Szikora I, Berentei Z, Kulcsar Z, et al. **Treatment of intracranial aneurysms by functional reconstruction of the parent artery: the Budapest experience with the Pipeline embolization device.** *AJNR Am J Neuroradiol* 2010;31:1139–47 [CrossRef Medline](#)
5. Lylyk P, Miranda C, Ceratto R, et al. **Curative endovascular reconstruction of cerebral aneurysms with the Pipeline embolization device: the Buenos Aires experience.** *Neurosurgery* 2009;64:632–42; discussion 642–43; quiz N6 [CrossRef Medline](#)
6. Grunwald IQ, Kamran M, Corkill RA, et al. **Simple measurement of aneurysm residual after treatment: the SMART scale for evaluation of intracranial aneurysms treated with flow diverters.** *Acta Neurochir (Wien)* 2012;154:21–26; discussion 26 [CrossRef Medline](#)
7. Ionita CN, Paciork AM, Dohatcu A, et al. **The asymmetric vascular stent efficacy in a rabbit aneurysm model.** *Stroke* 2009;40:959–65 [CrossRef Medline](#)
8. Benz T, Kowarschik M, Endres J, et al. **A Fourier-based approach to the angiographic assessment of flow diverter efficacy in the treatment of cerebral aneurysms.** *IEEE Trans Med Imaging* 2014;33:1788–802 [CrossRef Medline](#)
9. Mut F, Ruijters D, Babic D, et al. **Effects of changing physiologic**

**conditions on the in vivo quantification of hemodynamic variables in cerebral aneurysms treated with flow diverting devices.** *Int J Numer Method Biomed Eng* 2014;30:135–42 [CrossRef Medline](#)

10. Morales HG, Bonnefous O. **Peak systolic or maximum intra-aneurysmal hemodynamic condition? Implications on normalized flow variables.** *J Biomech* 2014;47:2362–70 [CrossRef Medline](#)
11. Morales HG, Bonnefous O. **Modeling hemodynamics after flow diverter with a porous medium.** In: *Proceedings of the International Symposium on Biomedical Imaging*, Beijing, China. April 29 to May 2, 2014
12. Morales HG, Bonnefous O. **Unraveling the relationship between arterial flow and intra-aneurysmal hemodynamics.** *J Biomech* 2015;48:585–91 [CrossRef Medline](#)
13. Morales HG, Larrabide I, Geers AJ, et al. **Newtonian and non-Newtonian blood flow in coiled cerebral aneurysms.** *J Biomech* 2013;46:2158–64 [CrossRef Medline](#)
14. Bonnefous O, Pereira VM, Ouared R, et al. **Quantification of arterial flow using digital subtraction angiography.** *Med Phys* 2012;39:6264–75 [CrossRef Medline](#)
15. Pereira VM, Bonnefous O, Ouared R, et al. **A DSA-based method using contrast-motion estimation for the assessment of the intra-aneurysmal flow changes induced by flow diverter stents.** *AJNR Am J Neuroradiol* 2013;34:808–15 [CrossRef Medline](#)
16. Pereira VM, Ouared R, Brina O, et al. **Quantification of internal carotid artery flow with digital subtraction angiography: validation of an optical flow approach with Doppler ultrasound.** *AJNR Am J Neuroradiol* 2014;35:156–63 [CrossRef Medline](#)
17. Ford MD, Alperin N, Lee SH, et al. **Characterization of volumetric flow rate waveforms in the normal internal carotid and vertebral arteries.** *Physiol Meas* 2005;26:477–88 [CrossRef Medline](#)
18. Hoi Y, Wasserman BA, Xie YJ, et al. **Characterization of volumetric flow rate waveforms at the carotid bifurcations of older adults.** *Physiol Meas* 2010;31:291–302 [CrossRef Medline](#)
19. Cebal JR, Castro MA, Putman CM, et al. **Flow-area relationship in internal carotid and vertebral arteries.** *Physiol Meas* 2008;29:585–94 [CrossRef Medline](#)
20. Fernández MA, Gerbeau J, Martin V. **Numerical simulation of blood flows through a porous interface.** *ESAIM: Mathematical Modelling and Numerical Analysis* 2008;42:961–90 [CrossRef](#)
21. Augsburg L, Reymond P, Rufenacht DA, et al. **Intracranial stents being modeled as a porous medium: flow simulation in stented cerebral aneurysms.** *Ann Biomed Eng* 2011;39:850–63 [CrossRef Medline](#)
22. Zhang Y, Chong W, Qian Y. **Investigation of intracranial aneurysm hemodynamics following flow diverter stent treatment.** *Med Eng Phys* 2013;35:608–15 [CrossRef Medline](#)
23. Levitt MR, McGah PM, Aliseda A, et al. **Cerebral aneurysms treated with flow-diverting stents: computational models with intravascular blood flow measurements.** *AJNR Am J Neuroradiol* 2014;35:143–48 [CrossRef Medline](#)
24. Geers AJ, Larrabide I, Morales HG, et al. **Approximating hemodynamics of cerebral aneurysms with steady flow simulations.** *J Biomech* 2014;47:178–85 [CrossRef Medline](#)
25. Kim M, Taulbee DB, Tremmel M, et al. **Comparison of two stents in modifying cerebral aneurysm hemodynamics.** *Ann Biomed Eng* 2008;36:726–41 [CrossRef Medline](#)
26. Larrabide I, Geers AJ, Morales HG, et al. **Change in aneurysmal flow pulsatility after flow diverter treatment.** *Comput Med Imaging Graph* 2016;50:2–8 [CrossRef Medline](#)
27. Peach TW, Ngoepe M, Spranger K, et al. **Personalizing flow diverter intervention for cerebral aneurysms: from computational hemodynamics to biochemical modeling.** *Int J Numer Method Biomed Eng* 2014;30:1387–407 [CrossRef Medline](#)
28. Dempere-Marco L, Oubel E, Castro MA, et al. **CFD analysis incorporating the influence of wall motion: application to intracranial aneurysms.** *Med Image Comput Comput Assist Interv* 2006;9(pt 2):438–45 [Medline](#)